Appl. Phys. A 64, 127–137 (1997)

Applied Physics A Materials Science & Processing

© Springer-Verlag 1997

Invited paper

Gettering of metallic impurities in photovoltaic silicon

S.A. McHugo, H. Hieslmair, E.R. Weber

Department of Materials Science and Mineral Engineering, University of California at Berkeley, Berkeley, CA, USA 94720
(Fax: 001-510/42-2069, E-mail: sam@garnet.berkeley,edu; hhiesl@argon.eecs.berkeley.edu; weber@garnet.berkeley.edu)

Received: 21 June 1996/Accepted: 2 September 1996

Abstract. This work addresses the issue of structural defect-metallic impurity interactions in photovoltaic silicon and their effect on minority carrier diffusion length values. Aluminium and phosphorus segregation gettering studies were performed on photovoltaic silicon in order to gain insight into these interactions and quantify the effect of gettering on solar cell performance. Integrated circuit grade silicon was also studied for comparative purposes. Additionally, a novel rapid thermal annealing technique, designed to dissolve metallic impurity precipitates, and Deep Level Transient Spectroscopy were utilized to determine the as-grown impurity concentration in both grades of materials. Significant differences in gettering responses between the two grades of silicon are observed. Gettering treatments greatly improve I.C. grade silicon with a specific gettering temperature providing the optimal response. Photovoltaic grade silicon does not respond as well to the gettering treatments and, in some cases, the material degrades at higher gettering temperatures. The degradation is primarily observed in dislocated regions of multicrystalline photovoltaic silicon. Additionally, these dislocated regions were found to possess the highest as-grown metallic impurity concentration of all the materials studied. The dislocation-free photovoltaic silicon has a higher diffusion length relative to dislocated silicon but could not be improved by the gettering methods employed in this study. A model is presented to describe these phenomena where the high concentration of metallic impurities at dislocations produce relatively low minority carrier diffusion lengths as well as the degrading response with higher gettering temperatures while microdefects create an upper limit to the photovoltaic grade material's diffusion length.

PACS: 61.70; 81.40; 82.20

In order to lessen the environmental deterioration caused by fossil fuel and nuclear power plants, a variety of clean energy sources have been studied and partially implemented. Terrestrial solar cells are an excellent means to provide clean energy. Based on cost and solar cell efficiencies, silicon is one of the most promising materials for this application with the silicon being photovoltaic (solar) grade in multicrystalline (polycrystalline) or single crystal forms. The materials are typically grown 300–500 μm thick in order to absorb the majority of the Sun's radiation. This radiation absorption produces excess minority carriers in the material's bulk far from the current creating n^+-p junction which necessitates long minority carrier diffusion lengths (L_n) in these materials. In general, once the material's L_n becomes comparable to the solar cell thickness then all light generated carriers will be safely collected at the n^+-p junction and the cell's maximum power can be realized. Below this value the cell efficiency is drastically affected. L_n values of as-grown solar grade silicon are regularly under the cell thickness which necessitates steps for material improvement.

Metallic impurities and structural defects, specifically grain boundaries, dislocations and microdefects are the most conceivable sources for low L_n values in solar grade materials. Commonly present matallic impurities are Fe, Cu, Cr, Ti, and V in either dissolved or precipitated states. However, these impurities are generally not found dissolved in high enough concentrations to explain the measured low diffusion length values [1] and the material's as-grown L_n values are related to structural defects, not impurities [2, 3] in both single crystal and multicrystalline (mc-) silicon. While grain boundaries act as carrier recombination centers, their effect on L_n in mc-silicon is minimal due to the large grain size relative to the required L_n. Dislocations in mc-silicon can be found in very high concentrations, $> 10^8/cm^2$ and can have a significant impact on solar cell performance [4, 5]. Past work has shown that the carrier recombination activity at dislocations is primarily due to the presence of metallic impurities [6–13]. Thus, removal of metallic impurities from dislocations in mc-silicon is crucial. Microdefects in single crystal and mc-silicon have shown to be carrier recombination sites especially after decoration/precipitation with metallic impurities [14, 15]. Additional studies have strongly suggested these microdefects may influence L_n values, especially in materials with high as-grown L_n values [2, 3]. As with dislocations in mc-silicon, it is

imperative to remove metallic impurities from microdefects in single crystal and mc-silicon.

An effective means to remove metallic impurities and augment the material's L_n is via gettering. Standard solar cell processing steps intrinsically possess gettering capabilities. For instance, the p-n junction formation generally consists of a phosphorus in-diffusion which has been regularly observed to getter metallic impurities [1, 16–23]. Additionally, the aluminium backside sintering which forms the ohmic backside contact is also a means for metallic impurity gettering [20, 21, 23–26]. These processing steps should remove a significant amount of impurities and improve cell performance. However, full realization of this expectation has not occurred [3, 5, 21, 24, 27].

This work addresses metallic impurity-structural defect interactions in solar grade silicon. The focus is to understand the effect dislocations and microdefects have on gettering of metallic impurities in multicrystalline silicon particularly in regions of low minority carrier lifetime. Quantitative results of gettering efficiency in solar and I.C. grade silicon are presented as well as structural defect and metallic impurity chracterization. With these results, a model is proposed to explain segregation gettering in both solar and I.C. grade silicon.

1 Experimental

The solar grade materials used in this work were obtained from a variety of solar cell manufacturers. CZ solar grade silicon from two different manufacturers (denoted as solar CZ I and II) were included as well as ribbon grown mc-silicon (denoted as ribbon) from one manufacturer and cast mc-silicon (denoted as cast, I, II and III) from three different manufactures. I.C. grade FZ and CZ were used for comparison.

The solar CZ I silicon had an oxygen concentration of $\approx 10^{18}\,cm^{-3}$, a carbon concentration of $< 10^{16}\,cm^{-3}$ and a resistivity of 1–3 Ω-cm. Two types of solar CZ II were available for this study which are differentiated by their carbon concentrations. One is of low carbon content, $< 10^{16}\,cm^{-3}$, and the other high carbon content, $\approx 2\times10^{17}\,cm^{-3}$. Both types possessed oxygen concentrations of $\approx 9\times10^{17}\,cm^{-3}$ and resistivities of 0.8–1.5 Ω cm. The ribbon and cast I materials had oxygen concentrations of $< 10^{17}\,cm^{-3}$, carbon concentrations of $\approx 8\times10^{17}\,cm^{-3}$ and $< 10^{17}\,cm^{-3}$, respectively, with resistivities of 2-5 Ω-cm each. The case II and III materials contained oxygen concentrations of $< 10^{17}\,cm^{-3}$ and $\approx 8\times10^{17}\,cm^{-3}$, respectively, carbon concentrations of $< 5\times10^{17}\,cm^{-3}$ with resistivities of ≈ 0.6 and 1–1.7 Ω-cm, respectively. The I.C. grade FZ and CZ both had carbon concentrations, $< 10^{16}\,cm^{-3}$, while the CZ material possessed an oxygen concentration of $\approx 9\times10^{17}\,cm^{-3}$. Resistivities were 6.2–8.5 Ω-cm for the FZ and ≈ 10 Ω-cm for the CZ. For the mc-silicon, samples with the same grain structure, i.e. along the growth direction, were used. This sample selection allowed for accurate comparisons of material responses to various treatments. This is key for studies of mc-silicon because microstructure and properties can vary greatly across the material.

Samples from all materials were subjected to a standard cleaning process prior to all annealings, Surface Photovoltage (SPV) and Fourier Transform Infrared Spectroscopy (FTIR) measurements, preferential etchings and diode formation steps. The process began with solvent cleaning followed by a piranha cleaning (5:H_2SO_4, 1:H_2O_2@ 120°C) in a high purity VLSI grade sink. After a de-ionized H_2O rinse, the samples received a short HF dip to remove any oxide and a mild silicon etch to remove 0.1–0.3 μm.

Intentional Fe contamination was accomplished with the evaporation of high purity Fe onto the samples' backsides using a thermal evaporator at vacuum pressures of $2–4\times10^{-7}$ torr. Upon annealing, this Fe reacted with the silicon to form $FeSi_2$ from which Fe was driven into the silicon. The indiffusion temperature determined the concentration of Fe by equilibration of $FeSi_2$ with the silicon [28]. All samples were annealed in a nitrogen atmosphere for sufficient time to guarantee uniform distribution of Fe throughout the material, after which the samples were quenched into ethylene glycol (≈ 1000 K/s) to room temperature. Deep Level Transient Spectroscopy (DLTS) was performed on select samples to quantify the concentration of introduced Fe. Residual Fe and $FeSi_2$ on the sample's surface was removed by polishing and a 5–10 μm silicon etch.

All gettering anneals were performed in furnaces used daily for I.C. device fabrication, ensuring clean processes. For A1 gettering, first a high purity A1 layer was sputtered onto the sample backside, then the samples were annealed in an A1 sintering furnace. Phosphorus gettering utilized a $POCl_3$ atmosphere in a furnace specifically used for phosphorus in-diffusion. After the gettering anneals the phosphorus glass layer and phosphorus in-diffused region were removed with a silicon etch (2 HNO_3:1 CH_3OCH:1 HF) which removed approximately 5–10 μm while the A1 layer was etched away with a metal etchant. An additional 5–10 μm was removed with a silicon etch to ensure all A1 doped silicon was removed.

Rapid Thermal Annealing (RTA) treatments were conducted in a commercially available system. All RTA treatments were carried out in a nitrogen atmosphere at 1100 °C for 45 seconds. Following the RTA treatment, the samples were slowly cooled in a nitrogen atmosphere, reaching 500 °C within approximately 1 min and 300 °C in 5 min. RTA Quenching (RTAQ) treatments were carried out with a custom built system which consists of two vertically opposed heat lamps, similar to those used in commerically available RTA systems. The sample is held vertically by two mobile quartz rods inside a quartz tube through which nitrogen gas flows. This configuration allows for a rapid quench of the sample into ethylene glycol after the appropriate anneal. A quench rate of 1000 K/s has been estimated for this procedure. All anneals were conducted at 1100 °C for either 45 s or 4 min.

Since increases in minority carrier diffusion length (L_n) are the primary benefit from gettering treatments, Surface Photovoltage (SPV) measurement of L_n were used to quantify the gettering response in this study. This is a standard technique for measurement of diffusion length [29–31].

In order to assess the quantity and type of metallic impurities in the various silicon materials, Deep Level Transient Spectroscopy (DLTS) with aluminum Schottky diodes was utilized. DLTS is a highly sensitive technique for impurity detection. Typical sensitivity limits are on the order of 10^{11} impurity atoms/cm^3 for the materials used in this study.

Oxygen concentrations were measured using Fourier Transform Infrared Spectroscopy (FTIR) before and after annealing treatments [32]. With these measurements and subsequent calculations using Ham's law [33] and mass conservation, the oxygen precipitate density and radius were quantified.

The defect structure of the various materials was determined with sample polishing, preferential etching and surface analysis. Polishing with 1200, 2400 and 4000 grit polishing paper and 1.0, 0.3 and 0.05 μm Al_2O_3 polishing powders produced mirror-like surfaces. A Schimmel preferential etch [34] was used to reveal grain boundaries, dislocations and microdefects as stipulated in [35, 36]. The etch pits were observed with a Scanning Electron Microscope (SEM) in secondary electron imaging mode. Defect concentrations were calculated by simply counting etch pits over a wide area, typically mms in scale.

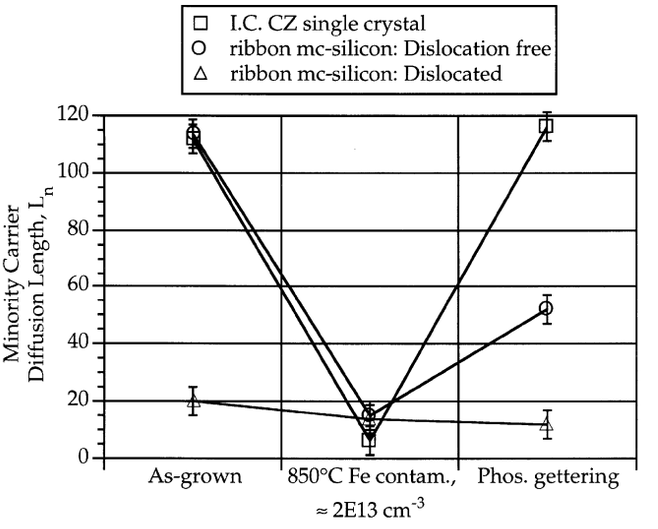

Fig. 1. Integrated circuit (I.C.) grade CZ, dislocated and dislocation-free ribbon mc-silicon responses to iron contamination and phosphorus gettering. Phosphorus gettering was carried out in a two step process: 1–900 °C for 2 hrs in a $POCl_3$ atmosphere, 2–700 °C for 2 hrs in a nitrogen atmosphere

2 Results

2.1 Phosphorus gettering of intentionally contaminated silicon

The effect of metallic impurities on the material's performance was revealed by intentional Fe contamination of I.C. grade single crystal silicon and solar grade mc-silicon followed by phosphorus gettering to remove the iron. The phosphorus gettering was carried out in a two step thermal treatment: a 2 hour $POCL_3$ in-diffusion at 900 °C followed by a 2 hour 700 °C treatment in N_2 atmosphere. It should be noted that the phosphorus gettering treatment employs a slow temperature ramp (20 min) from 700 °C to the intended 900 °C annealing temperature which allows for Fe precipitation. The material's minority carrier diffusion length (L_n), as measured by the Surface Photovoltage technique (SPV), was used as a figure of merit for the material's performance. The comparison between I.C. grade and solar grade silicon was included to elucidate any differences between the material's gettering behavior.

Figure 1 shows a result of this study on I.C. grade CZ silicon and both a high dislocation density (5×10^7/cm^2) and a dislocation-free sample of the ribbon mc-silicon. The carrier diffusion length is given after each stage of sample treatment. The sample's as-grown diffusion length is shown on the left side. We see the dislocated material's as-grown diffusion length is significantly lower than the dislocation-free ribbon silicon and the I.C. grade CZ. Of particular interest is that the dislocation-free material's as-grown diffusion length is comparable to the I.C. grade CZ. Following the introduction of Fe at 850 °C, corresponding to 2×10^{13} Fe-B pairs/cm^3 as confirmed by Deep Level Transient Spectroscopy (DLTS), each material's diffusion length plummeted to 15–20 μm as shown in the middle of Fig. 1. It should be noted that Fe pairs with boron within hours after the in-diffusion [37, 38]. Diffusion lengths after phosphorus gettering are shown on the right side of Figure 1. Here we see the I.C. grade CZ returned to its original L_n value, indicating all introduced impurities were removed. However, for the ribbon material, the L_n value did not significantly improve. Most noticeably, the dislocation-free material did not return to its original L_n value. These results are the first indication that phosphorus gettering (a standard I.C. gettering procedure) does not improve solar grade mc-silicon as well as I.C. grade single crystal silicon.

DLTS measurements, performed after the phosphorus gettering treatment, indicated no dissolved impurities were present in any of the materials. This is not surprising since, after the phosphorus gettering treatment, the samples are slowly cooled which necessitates precipitation of fast diffusing impurities such as Fe and Cr. However, slow diffusing impurities, such as Ti, V and Mo would not be expected to appreciably precipitate. Therefore, these measurements indicate that slow diffusers are not present in these materials.

Microstructural analysis after this gettering treatment did not reveal microdefects, indicating they are not heavily decorated with impurities as required for detection [2, 15]. However, limited impurity decoration or precipitation of the Fe at microdefects may have occurred.

An extension of the above mentioned study was to determine the effect of impurity concentration to gettering response in both I.C. and solar grade materials. Figure 2 shows the L_n response of dislocated ribbon mc-silicon ($\approx 10^7$/cm^2) and high purity FZ subjected to varying amounts of intentional Fe contamination. The left size of Fig. 2 shows the material's as-grown diffusion length. We see the FZ silicon possesses a significantly higher L_n than the ribbon mc-silicon and even the I.C. CZ from Fig. 1.

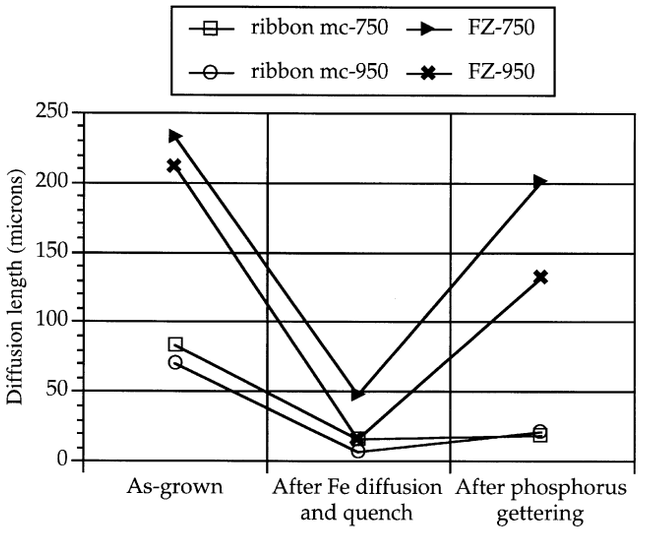

Fig. 2. FZ and dislocated ribbon mc-silicon responses to a range of iron concentrations and phosphorus gettering. Phosphorus gettering was carried out in a two step process: 1–900 °C for 2 hours in a $POCl_3$ atmosphere, 2–700 °C for 2 hrs in a nitrogen atmosphere

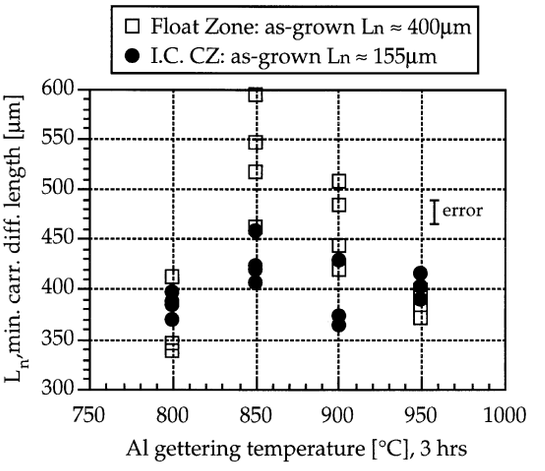

Fig. 3. Temperature dependent gettering for I.C. grade silicon

This is as expected since this is high purity FZ with low impurity and defect densities.

Iron introduction was carried out at 750 °C and 950 °C corresponding to a low ($\approx 2 \times 10^{12}$ Fe atoms/cm^3) and a high (2×10^{14} Fe atoms/cm^3) contamination level, respectively. The diffusion length values indicate more impurities were incorporated during the 950 °C in-diffusion, as expected.

Following phosphorus gettering, a large improvement in L_n was observed in the FZ material. For the ribbon mc-silicon, no response to the gettering was observed for either the low or high contamination levels. This is similar to the response observed for the dislocated sample in Figure 1 where phosphorus gettering is shown to be inadequate for impurity removal from solar grade mc-silicon.

2.2 Aluminum gettering of as-grown silicon

2.2.1 Temperature dependence. The influence of temperature on the material's gettering response was studied for both I.C. grade and solar grade materials. Considering segregation-induced gettering as a three step process of impurity release, diffusion and capture, a model has been proposed to describe the temperature dependence of gettering efficiency [18]. The gettering process is limited by release or diffusion of the impurity at low temperatures and capture of the impurity at higher temperatures. This creates an optimal gettering temperature. Extrapolating from this model and considering the capture limited case is thermodynamically defined while the diffusion or release limited cases are kinetically defined, a time dependent gettering response would be expected for the release/diffusion limited region. A maximum gettering efficiency will be reached after extended gettering times when all impurities have been removed. At lower temperatures this maximum gettering efficiency is attained after even longer times.

With the above mentioned model, one can qualitatively understand fundamental aspects of materials by analyzing their gettering response with varying temperatures. Based on this understanding, aluminum gettering was conducted on a variety of I.C. and solar grade silicon. Each sample was annealed at 800, 850, 900 and 950 °C for 3 hours with a 2.5 μm thick layer of A1 on the sample's backside. All samples were in their as-grown state with no intentional contamination.

The results for I.C. grade silicon are shown in Fig. 3. The diffusion length (L_n) for each material after the gettering anneal is plotted versus the gettering temperature. As-grown diffusion lengths are given in the legend at the top of the graph. We see the gettering sequence has greatly increased the CZ material's L_n value at all temperatures while the FZ material's has only slightly increased. Additionally, an optimal temperature is observed for both materials at ≈ 850 °C. This is in agreement with the above mentioned model.

Solar grade silicon was also subjected to varying A1 gettering temperatures. This included both single crystal CZ and mc-silicon. Figure 4 displays the results for the single crystal solar grade CZ. The material's initial L_n is shown on the graph's right hand side. Two types of responses are observed. The solar CZ I material's L_n was unaffected by any of the gettering treatments while both solar CZ II material's L_n degraded from their initial L_n to a greater degree as the gettering temperature was increased. Both of these responses are significantly different than the I.C. grade silicon's response in Fig. 3 which once more suggests these grades of materials respond differently to gettering treatments.

Deep Level Transient Spectroscopy (DLTS) measurements on these materials in their as-grown and post-gettering state did not reveal any majority carrier traps such that slow diffusing impurities line Ti, V and Mo are not present in appreciable concentrations. Microstructural analysis uncovered shallow etch pits in each material which are characteristically associated with oxygen precipitates. An example of these etch pits is shown in Fig. 5.

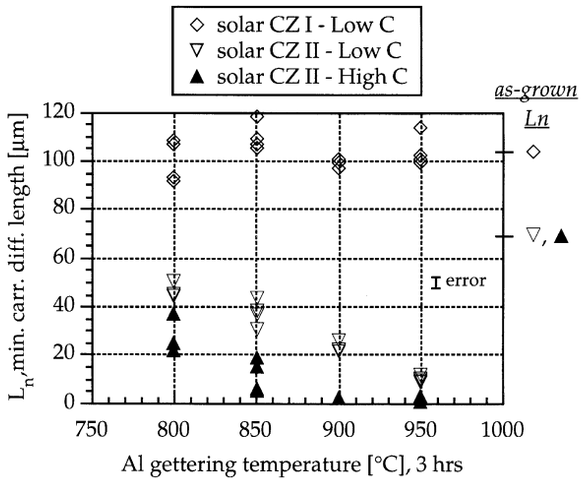

Fig. 4. Temperature dependent gettering for as-grown solar CZ I and II material

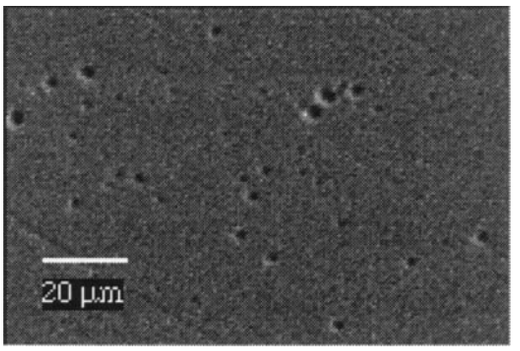

Fig. 5. SEM micrographs of as-grown solar CZ II following preferential etching. Shallow etch pits are associated with microdefects in the materials

Figure 6 shows the response of both the ribbon and cast I mc-silicon to gettering temperature was similar to that of solar grade CZ. Regions 5 and 6 of the ribbon material are invariant to gettering temperature while regions 1–4 and the cast mc I materials degrade with increasing temperature.

Microstructural analysis of these materials after gettering revealed the following: region 6 is approximately dislocation free, region 5 has a low dislocation density ($< 10^4$ cm^{-2}) and regions 1–4 possess significantly higher dislocation densities, from 10^7 to 10^9 cm^{-2}. A micrograph of a very high dislocation density sample is given in Fig. 7. Additionally, all the cast I samples have dislocation densities of $\approx 10^7$ cm^{-2}. Thus, in mildly to highly dislocated materials, a degrading gettering response is observed while in relatively dislocation-free material an invariant response is found. This agrees with other work [4] which showed the L_n of mc-silicon is significantly lowered only when the dislocation density is greater than 10^5 cm^{-2}. It is important to note that microdefects were not detected with this microstructural analysis after gettering or in the as-grown state which suggests they are not as heavily decorated as were the microdefects in [2, 15].

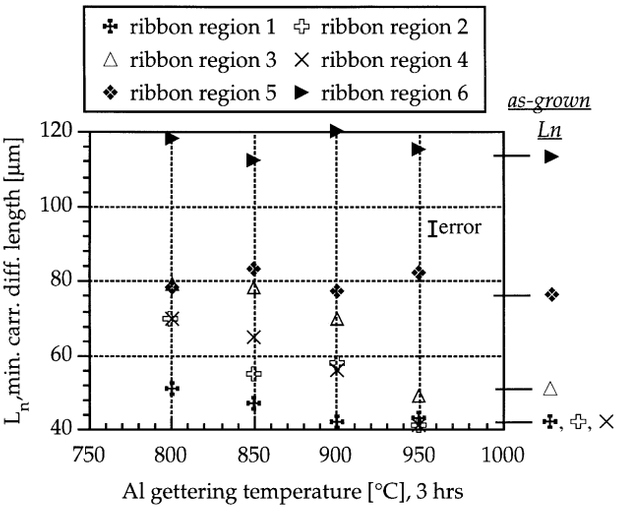

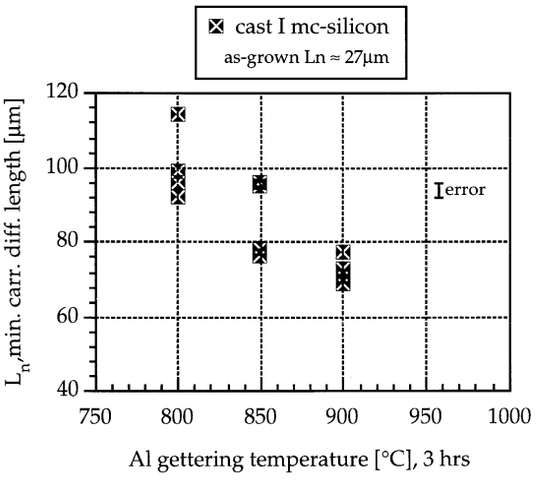

Fig. 6. Temperature dependent gettering for as-grown ribbon mc-silicon and cast I mc-silicon

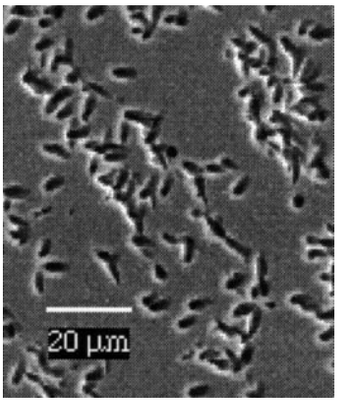

Fig. 7. SEM micrograph of high dislocation density ribbon mc-silicon. Etch pits are associated with dislocations

DLTS measurements on ribbon regions 1–6 and the cast I materials did not detect any majority carrier traps. Thus, typical slow diffusers, such as Ti, V and Mo, are not present in any significant amount in these materials.

2.2.2 Time and Aluminum Layer Thickness Dependence. The influence of gettering time and gettering layer thickness on the material's gettering response was studied for solar grade materials. These experiments are designed to determine whether the gettering of solar grade materials is limited kinetically or thermodynamically. The aluminum layer thickness influences the thermodynamics of the gettering process via the effective gettering coefficient which is defined as the ratio of initial to final impurity concentration in the silicon matrix for an impurity. It is derived from conservation of mass and the definition of the segregation coefficient, S:

$$\frac{C_{\text{imp}-\text{Si}}}{C_{\text{imp}-\text{Si}_0}} = \frac{t_{\text{Si}}}{t_{\text{Si}} + St_{\text{Al}}} \tag{1}$$

where $C_{\text{imp}-\text{Si}}$ is the impurity concentration in the silicon after gettering, $C_{\text{imp}-Si_0}$ denotes the initial impurity concentration in the silicon and t is thickness. S is the ratio of an impurity specie in the gettering layer to that in the silicon matrix which can be estimated as 10^5–10^6 by considering the maximum solubility fot metallic impurities in silicon [28] and the solubility of metallic impurities in Al and Al-Si [39, 40]. From Eq. 1, it is apparent that a thicker aluminum layer will remove more impurities from the silicon. Again, this assumes the process is limited thermodynamically, not kinetically.

Aluminum gettering on as-grown solar grade materials was carried out for 1, 3 and 5 h at 850 °C with either a 2.5 μm or 0.25 μm thick layer of aluminum on the samples backside. These different thickness' allow for the possibility of an order of magnitude difference in post-gettering impurity concentrations form Eq. 1. The same material as studied in the temperature dependent study was used, allowing for accurate comparison.

Figure 8 shows the time and thickness dependence for solar CZ I and II materials. The y-axis denotes the L_n value after gettering. We see the solar CZ I and the high carbon solar CZ II materials gettering responses did not vary for any thickness or gettering anneal time. The solar CZ I materials retained its initial L_n value while the high carbon solar CZ II material degraded significantly from its initial value, just as in the temperature dependent study. However, the low carbon solar CZ II L_n value shows a kinetic degradation between the first 1–3 hrs after which its stabilizes at a low L_n value.

Varying gettering times and aluminum thickness' was also performed on ribbon regions 1–4. No significant change in gettering response is apparent for any of the regions. It must be noted that dislocation climb should be active at 850 °C and should continue with increasing time. This dislocation motion should increase lattice disorder which could degrade L_n. This is not observed.

2.3 RTA and RTAQ pretreatments

With high temperature treatments, impurity precipitates should dissolve into the material and/or impurities would be rapidly released from their previous site. In turn, the aluminum gettering treatments would be more effective since the barrier for dissolution or release would have

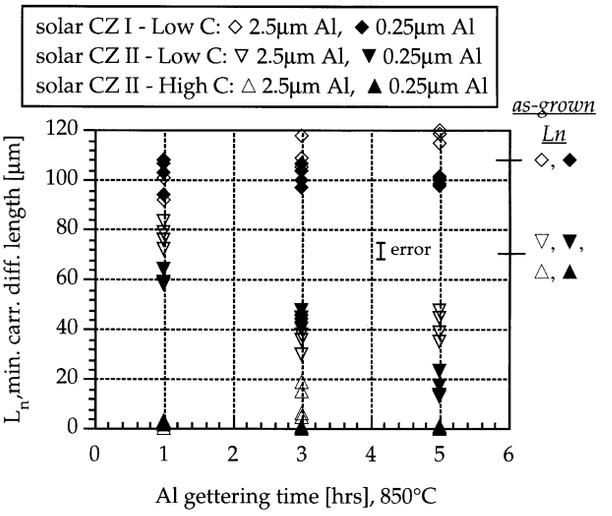

Fig. 8. As-grown solar CZ I and II gettering response dependence on gettering time and aluminum layer thickness

already been circumvented. Based on this premise, RTA and RTAQ heat treatments at 1100 °C for 45 s were applied to I.C. and solar grade materials prior to a 900 °C, 3 h aluminum gettering treatment. The RTA treatments have a slow cool after the high temperature treatment while the RTAQ treatments have a rapid quench. The slow cool may allow for some impurity precipitation. Although precipitation cannot be avoided during the initial stages of the subsequent aluminum gettering, some difference was expected between the two pre-treatments.

The results for I.C. and solar grade CZ are shown in Fig. 9. The y-axis displays L_n values in the as-grown state, after only Al gettering, after RTA/Al gettering and after RTAQ/Al gettering treatments. The I.C. CZ has a slightly decreased final L_n value with RTA and RTAQ treatments as compared with Al gettering only. Although the L_n value has increased drastically from the as-grown value, it seems the improvement originates from the Al gettering. The solar CZ I material is unaffected by the RTA process while the RTAQ process has slightly decreased the L_n response to aluminum gettering. Conversely, the solar CZ II materials shows dramatic improvement in L_n values with both RTA and RTAQ processes. The treatments retain the material's as-grown L_n values while Al gettering alone degrades the material. Apparently the RTA and RTAQ treatments remove this degrading mechanism which, from the above temperature dependent results, is stable up to 950 °C.

In order to determine the influence of oxygen precipitation on L_n degradation in solar CZ II silicon, Fourier Transform Infrared Spectroscopy (FTIR) was used to measure interstitial oxygen (O_i) concentration in these materials. The O_i results, shown in the first column of Table 1, reveal a significant amount of oxygen has precipitated after the 900 °C/3 hr A1 gettering anneal, especially in the high carbon material. More importantly, it is apparent that less oxygen precipitation occurs when either a RTA or RTAQ pretreatment is employed, suggesting these pretreatments have dissolved oxygen precipitate

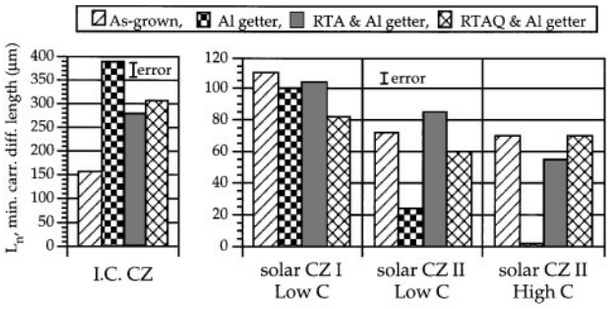

Fig. 9. RTA & RTAQ (1100 °C for 45 seconds) with aluminum gettering (900 °C for 3 hrs) results for I.C. CZ and solar grade CZ I and II

nuclei such that during the Al gettering treatment the density of large oxygen precipitates does not increase significantly. High temperature treatments, in the range of 1000 °C and up, have been used to dissolve oxygen precipitate nuclei sites, [41–45], supporting this model. Similar analysis on solar CZ I material revealed little or no oxygen had precipitated during the 900 °C/3 hr Al gettering anneal. Considering this material has approximately the same initial interstitial oxygen concentration as the solar CZ II materials, it seems the density of oxygen precipitate nuclei is the critical factor in regards to solar CZ degradation.

To quantify the effect of the RTA/RTAQ pretreatments on oxygen precipitate densities (n) and radii (r_0), Ham's law [33]:

$$nr_0 = \left(\frac{1}{4\pi D_{\mathrm{Oi}}}\right)\frac{1}{\tau} \tag{2}$$

and the mass-balance equation

$$[\Delta O_{\mathrm{i}}] = \left(\frac{4\pi r_o^3}{3}\right) nCp \tag{3}$$

were employed. Here D_{Oi} is the oxygen diffusivity at 900 °C (1.77×10^{-12} cm^2/s), ΔO_{i} is the drop in oxygen concentration, $C_{\mathrm{p}} = 4.65 \times 10^{22}$ oxy atoms in SiO_2/cm^3 and $1/\tau$ is the oxygen precipitation rate, found from:

$$[O_{\mathrm{i}}]_{\mathrm{final}} = [O_{\mathrm{i}}]_{\mathrm{initial}} \exp\left(\frac{-t}{\tau}\right) \tag{4}$$

The results of these calculations (Table 1) show that the RTA and RTAQ treatments reduce oxygen precipitate densities in both solar CZ II materials, especially in the high carbon content material. Moreover the density of oxygen precipitates is very high for all samples. In I.C. grade CZ silicon these densities can only be achieved with long, low temperature nucleation anneals [46–48]. In summation, these results indicate the degradation mechanism in solar CZ II materials is linked to a high initial oxygen precipitate nuclei density and their growth during the Al gettering anneal. The 1100 °C RTA and RTAQ pretreatments dissolve a significant number of oxygen precipitates which reduces oxygen precipitation and in turn arrests L_{n} degradation.

Figure 10 shows RTA/RTAQ results for regions 1–6 in the ribbon material. These regions possess the same grain structure as regions 1–6, respectively, in the temperature and time dependent studies where regions 1–4 are dislocated and regions 5–6 are relatively dislocation-free. From Fig. 10 we see small variations in L_{n} values with little or no consistency in dislocated and un-dislocated regions. The RTA and RTAQ treatments had little or no effect on the gettering response.

These RTA and RTAQ pre-treatments were also performed with cast II and III materials. The samples were selected in order to have correlated microstructures which allowed for accurate comparisons between treatments. High and low performance regions were selected from finished cells of each material type via Light Beam Induced Current (LBIC) images taken at Sandia National Laboratory. Results from the cast II material are given in Fig. 11. The first interesting fact from these data is the slight difference in as-grown L_{n} values between high and low performance regions. After Al gettering, we see a variety of L_{n} values. This is also seen with RTA and RTAQ pretreatments prior to Al gettering. Most regions only slightly change from their as-grown value while a few high performance regions slightly improve. This varying response to gettering is similar to ribbon mc-silicon where some regions were invariant to gettering while dislocated regions improve from their initial L_{n} value. Microstructural analysis of these materials shows both high and low performance regions have significant dislocation densities with the low performance regions having slightly higher densities.

Table 1. Interstitial oxygen concentrations [O_{i}], of high and low carbon content solar CZ II silicon. Oxygen precipitate densities and radii are calculated via Ham's law and mass conservation

Sample	Oxygen Conc, [O_{i}] (cm^{-3})	Precip. rate, $1/\tau$ (s^{-1})	nr_0 (cm^{-2})	Precipitate density, n (cm^{-3})	Precipitate radius, r_0 (nm)
as-grown High [C]	8.6×10^{17}	—	—	—	—
Al getter, High [C]	6.9×10^{17}	2.11×10^{-5}	9.5×10^{5}	9.72×10^{11}	9.76
RTA-Al getter, High [C]	8.3×10^{17}	3.84×10^{-6}	1.73×10^{5}	1.69×10^{11}	10.2
RTAQ-Al getter, High [C]	8.1×10^{17}	5.76×10^{-6}	2.59×10^{5}	2.55×10^{11}	10.2
as-grown, Iow [C]	9×10^{17}	—	—	—	—
Al getter, Low [C]	8.4×10^{17}	5.32×10^{-6}	2.39×10^{5}	2.31×10^{11}	10.4
RTA-Al getter, Low [C]	9.1×10^{17}	< 0	—	—	—
RTAQ-Al getter, Low [C]	8.6×10^{17}	3.59×10^{-6}	1.61×10^{5}	1.55×10^{11}	10.4

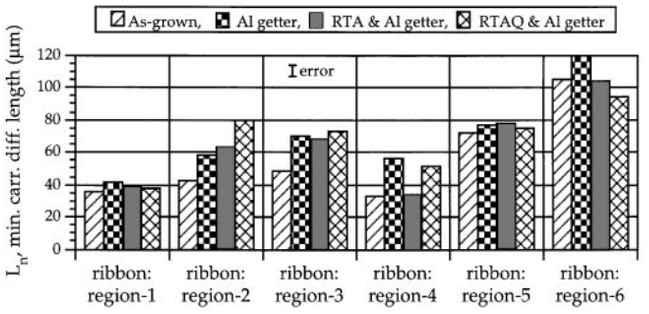

Fig. 10. RTA & RTAQ (1100 °C for 45 seconds) with aluminum gettering (900 °C for 3 hrs) results for as-grown ribbon mc-silicon. Regions 1–4 dislocation densities range from 10^7–10^9 cm^{-2} while regions 5&6 dislocation density is $< 10^4$ cm^{-2}

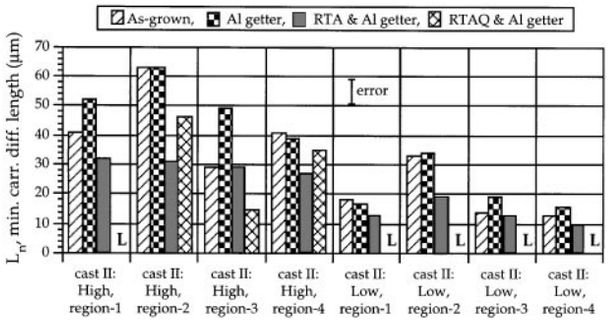

Fig. 11. RTA & RTAQ (1100 °C for 45 seconds) with aluminum gettering (900 °C for 3 hrs) results for as-grown cast II mc-silicon, both high and low cell performance regions. L denotes sample was lost during processing

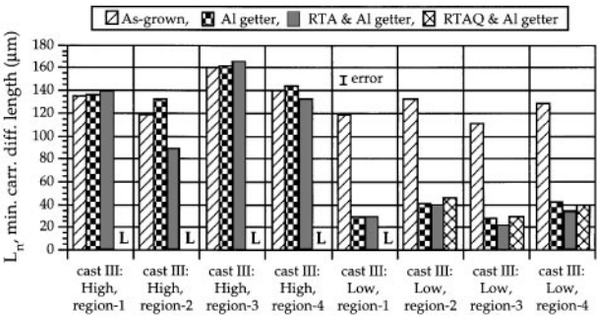

Fig. 12. RTA & RTAQ (1100 °C for 45 seconds) with aluminum gettering (900 °C for 3 hrs) results for as-grown cast III mc-silicon, both high and low cell performance regions. L denotes sample was lost during processing

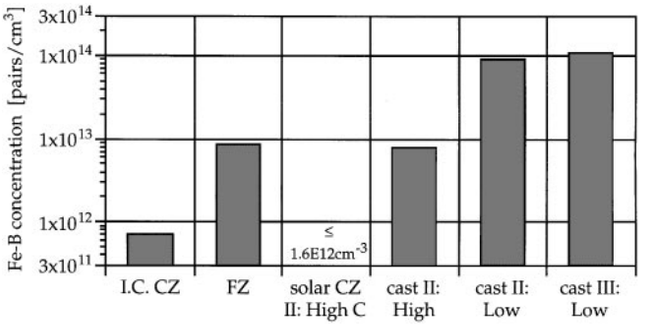

Fig. 13. RTAQ (1100 °C for 4 min)/DLTS results from as-grown FZ, I.C. grade CZ, high carbon content solar CZ II, high and low performance cast II mc-silicon and low performance cast III mc-silicon

Results from the cast III material are displayed in Fig. 12. Both high and low performance regions possess a high initial L_n value. The high performance materials are relatively unaffected by the Al gettering procedure while the low performance regions have seriously degraded. This same trend is realized for the samples subjected to RTA and RTAQ treatments prior to Al gettering. This result indicates the diffusion length limiting mechanism in this low performance cast III material is activated during the Al gettering step. This mechanism is not found in high performance regions. These cast III results are similar to those of the ribbon mc-silicon where a degradation or an invariance is observed depending on dislocation densities. A high dislocation density gives a degrading response and a relatively dislocation-free region gives an invariant response. Microstructural analysis of the cast III material reinforced this deduction. The high performance region possessed a low dislocation density while the low performance regions had a significantly higher dislocation density.

2.4 Initial impurity concentrations

In order to gain insight into initial impurity concentrations of these materials the following procedure was employed: a 1100 °C, 4 min RTAQ treatment followed by DLTS measurements. This procedure was used on the same I.C. and solar grade silicon as above, specifically, the FZ and I.C. CZ as well as high carbon solar CZ II, cast II material (high and low performance regions) and cast III material (low performance region). The concept was to dissolve all impurity precipitates and then measure impurity concentrations in each material. This would serve to elucidate models which describe the gettering behavior of each material.

The DLTS measurements only detected Fe in these materials. Since all materials are p-type, the Fe was found in the Fe-B state. The concentrations of Fe-B in each material are shown in Fig. 13. These numbers are an average of 3–4 measurements on various regions of each sample. A typical spread in data for one material type was $\pm$ 10%. The DLTS measurements were taken 10–25 μms below the sample surface for the FZ and I.C. CZ materials, by use of silicon etching, and $\approx$ 150 μm below the sample's surface for the solar CZ II, cast II and cast III samples by use of polishing and etching. We see that I.C. grade CZ possesses an extremely small impurity concentration, indicative of the cleanliness of the material and the RTAQ process. Surprisingly the FZ material has a significant Fe level, greater than the solar CZ II material. The detection limit for the solar CZ II material is high due to its low resistivity which limit the DLTS sensitivity. Of particular interest is the great variance in Fe

concentrations between high and low performance cast II materials. Specifically, low performance corresponds with a high Fe concentration. The low performance cast III materials has the highest Fe concentration of all the materials, indicating that Fe is linked to the poor gettering response in mc-silicon materials. Considering the microstructural analysis on these materials, which related low performance to high dislocation density, clearly there is a relation between iron concentrations and dislocation density. DLTS was also carried out on these low performance regions in their as-grown state. No impurities were revealed in either the as-grown cast II or III mc-silicon, indicating the Fe is released during the 1100 °C/4 min RTAQ treatment.

3 Discussion

3.1 Gettering: I.C. vs. solar grade silicon

In this study, significant differences in gettering response were realized for I.C. and solar grade silicon. Of particular interest are the results of Fig. 1 which reveal a fundamental difference in gettering of intentionally introduced iron between I.C. grade CZ and dislocated or dislocation-free solar grade mc-silicon. One would readily expect the dislocated mc-silicon to be gettered less efficiently than the I.C. material, however the dislocation-free mc-silicon should have responded in a manner comparable to the I.C. material. The most likely cause for this disparity would be a difference in the microdefects of I.C. CZ and mc-silicon. The total microdefect concentration in I.C. CZ is typically in the 10^5 to $10^8/cm^3$ range depending on growth conditions. Specific heat treatments can induce large oxygen precipitates and related defects with densities in 10^8 to $10^{10}/cm^3$ range [46–48]. Microdefects in mc-silicon generally range in concentrations from 10^{11} to $10^{12}/cm^3$ [2, 15]. Based on these facts one may suggest the great disparity in gettering response between I.C. CZ and dislocation-free solar grade mc-silicon originates from the large difference in microdefect concentrations. Moreover, considering the data of Table 1, the great difference in material performance between solar grade CZ and I.C. grade CZ may also be due to a large difference in as-grown oxygen precipitate densities. Considering the precipitate densities are greatly influenced by growth speed and temperature gradient at the solid/liquid interface, it seems that control of these parameters is crucial for growth of high quality solar grade CZ.

The large difference in gettering behavior between I.C. grade and solar grade material is also portrayed in Figs 3, 4 and 6. Here the temperature dependence of I.C. and solar grade materials differs greatly in the manner and the magnitude of the response. The I.C. material follows the model given by Kang and Schroder [18] with impurity diffusion limiting gettering at low temperatures and the thermodynamically defined segregation coefficient limiting gettering at higher temperatures. Contrasting the I.C. materials are the solar grade materials which either possess an invariant response to gettering temperature or a degrading response with increasing temperature. Additionally, the I.C. material's L_n after gettering is significantly higher than any of the solar grade materials even though the I.C. CZ material had an initial L_n comparable to some solar grade materials. As discussed below, the solar grade material's limitations can be explained by dislocations and microdefects and their interactions with metallic impurities. This hinders the gettering action and degrades the material's L_n.

3.2 Performance limitations in solar grade silicon

In this study, a variety of gettering treatments have been attempted to improve the minority carrier diffusion length in numerous solar grade silicon materials. Based on gettering temperature dependence of Figs 4 and 6, solar grade materials can be divided into two groups: invariant and degrading response. The invariant response is found in dislocation-free materials and the degrading response in dislocated materials. Solar CZ II materials are an exception where a high degree of oxygen precipitation correlates to material degradation, as shown in Table 1. This degradation relation to oxygen has been observed in other work [49]. The key parameters related to this material's degradation at high temperatures are initial oxygen concentration and initial oxygen precipitate nuclei density. The latter depends critically on the crystal's thermal history during growth.

The invariant materials do not respond to deviations in gettering temperature, time or thermodynamics (Figs 4, 6 and 8) nor to high temperature RTA/RTAQ pretreatments (Figs 9, 10). Considering these facts one may suggest that microdefects create an upper limit to the solar grade material's minority carrier diffusion length which cannot be improved via gettering treatments. The high microdefect concentration in solar grade silicon relative to I.C. silicon accounts for the great disparity in material performance. The microdefect recombination activity originates either intrinsically at the defect's surface or from metallic impurities decorating/precipitated at the defect. If metallic impurities are the case, the majority of the impurities do not release during typical gettering treatments due to stabilization of the impurities at the microdefect. This stabilization may originate from previous impurity chemisorption onto the microdefect, a surface energy reduction at the metallic impurity precipitate/microdefect interface or an earlier chemical surface reaction between the impurity and the microdefect. These mechanisms would be expected to significantly increase the impurity's enthalpy of formation between the microdefect and the surrounding silicon and, in turn, would drastically reduce the impurity's solubility in the silicon matrix. This would inhibit impurity release and thus present gettering.

The materials which degrade with increasing gettering temperature do not respond to variations in gettering time or thermodynamics (Fig. 8) nor to high temperature RTA/RTAQ pretreatments (Figs 9, 10), excluding the solar CZ II materials where significant oxygen precipitation is retarded with the pretreatments. Most importantly a correlation has been established between the degrading response and the dislocation density. Considering these facts, this degrading behavior can be understood by first

conceiving that high concentrations of impurities precipitate at or decorate dislocations in mc-silicon during the slow cool after crystal growth, as suggested by the RTAQ/DLTS results of Fig. 13. Essentially the dislocations act as a preferable precipitation site for metallic impurities. In dislocation-free regions, impurities diffuse either to these dislocated regions or to the surface where they are easily removed. The concept of a dominant precipitation site has been observed in past work on preferred impurity precipitation with slow cooling rates [15, 50]. In theory, these dislocated regions could have impurities dissolved or in precipitate form corresponding to concentrations of up to the impurity's solubility in silicon ($\approx 10^{18}$ cm^{-3} for some impurities).

Of course, the question for these dislocated mc-silicon materials is why they degrade with increasing gettering temperature. This can be understood if one considers that the gettering process does not run to completion for the times used in this study. With incomplete gettering, the impurities are left dispersed throughout the silicon lattice after the treatment. The temperature dependent degradation occurs because more impurities are left in the lattice at higher temperatures. The gettering could be incomplete for the following reasons: 1) The dislocations act as a fine dispersion of line sources for the impurities which requires significantly longer gettering times than gettering of a homogeneous distribution of dissolved impurities; 2) the high strain field of the dislocation, which has made it a preferable precipitation/decoration site during the slow cool from growth, conversely creates a more stable site for precipitates during gettering. This stabilization lowers the impurity's solubility in the silicon matrix relative to the dislocation such that the impurity flux from the dislocation to the gettering layer is drastically reduced and longer gettering times are necessary; 3) the metal impurities have reacted with other impurities, such as carbon or oxygen as suggested in [4], to form species which are more stable than metal silicides or agglomerates. Again with a more stable specie longer gettering times would be required. The latter two reasons indicate that gettering in mc-silicon is a release limited process.

4 Conclusions

The work presented here demonstrates a fundamental difference between I.C. and solar grade silicon in terms of their gettering response and gettering temperature dependence. These differences have been related to structural defects found in solar grade materials, specifically dislocations and microdefects, as well as the material's high impurity concentration. Dislocations severely degrade material performance through interactions with metallic impurities. A high density of microdefects in solar grade material creates an upper limit to its performance, leaving the material insensitive to the gettering treatments considered here. Furthermore, microdefects in the form of oxygen precipitates can degrade the material's performance during processing when present in high concentration via rapid oxygen precipitation.

Acknowledgements. The authors would like to thank S.M. Myers, F.G. Kirscht, J. Kalejs, A. Rohatgi, T. Tan, U. Gösele, W. Schröter and T. Heiser for many illuminating discussions. Special thanks goes to K. Schubert for the LBIC work performed at Sandia National Laboratories as well as J. Kalejs, M. Werner and C. Khattak for the supply of silicon materials. Additionally, many thanks goes to SDI for the SPV apparatus. This work was supported by NREL subcontract XD-2-11004-3.

References

1. L. Jastrzebski, W. Henley, D. Schielein, J. Lagowski: J. Elec. Chem. Soc. **142**, 3869 (1994)
2. J. Bailey, E.R. Weber: Phys. Stat. Sol. (a) **137**, 515 (1993)
3. S.A. McHugo, J. Bailey, H. Hieslmair, E.R. Weber: In *1994 First World Conference on Photovoltaic Energy Conversion,* Waikoloa, Hawaii, U.S.A., 1994, p. 1607
4. S. Pizzini, A. Sandrinelli, M. Beghi, D. Narducci, F. Allegretti, S. Torchio, G. Fabbri, G.P. Ottaviani, F. Demartin, A. Fusi: J. Elec. Chem. Soc. **135**, 155 (1988)
5. B.L. Sopori, L. Jastrzebski, T. Tan, S. Narayanan: In *Proceedings of the 12th European Photovoltaic Solar Energy Conference*, Netherlands, 1994, p. 1003
6. H. Alexander, C. Kisielowski-Kemmerich, E.R. Weber: Physica **116B**, 583 (1983)
7. E.R. Weber, H. Alexander: Journal de Physique **C4**, 319 (1983)
8. C. Cabanel, J.Y. Laval, J. Appl. Phys. **67**, 1425 (1990)
9. K. Weronek, J. Weber, A. Höpner, F. Ernst, R. Buchner, M. Stefaniak, H. Alexander: In *Defects in Semiconductors 16, International Conference on Defects in Semiconductors*, edited by G. Davies, G. Deleo and M. Stavola, Lehigh University, U.S.A., 1991, p. 1315
10. V. Higgs, E.C. Lightowlers, C.E. Norman, P. Kightley: In *Defects in Semiconductors 16, International Conference on Defects in Semiconductors*, edited by G. Davies, G. Deleo and M. Stavola, Lehigh University, U.S.A., 1991, p. 1309
11. V. Higgs, M. Kittler: Appl. Phys. Lett. **63**, 2085 (1993)
12. M. Kittler, W. Seifert V. Higgs: Phys. Stat. Sol. (a) **137**, 327 (1993)
13. T.S. Fell, P.R. Wilshaw, M.D.d. Coteau: Phys. Stat. Sol. (a) **138**, 695 (1993)
14. T.H. Wang, T.F. Ciszek, T. Schuyler: Solar Cells **24**, 135 (1988)
15. S.A. McHugo, W.D. Sawyer: Appl. Phys. Lett. **62(20)**, 2519 (1993)
16. L. Baldi, G.F. Cerofolini, G. Ferla, G. Frigerio: Phys. Stat. Sol. (a) **48**, 523 (1978)
17. L. Baldi, G. Cerofolini, G. Ferla: J. Elec. Chem. Soc. **127**, 164 (1980)
18. J.S. Kang, D.K. Schroder: J. Appl. Phys. **65**, 2974 (1989)
19. W. Schröter, R. Kühnapfel: Appl. Phys. Lett. **56**, 2207 (1990)
20. P. Sana, J. Salami, A. Rohatgi: IEEE Transactions on Electron Devices **40**, 1461 (1993)
21. M. Loghmarti, R. Stuck, J.C. Muller, D. Sayah, P. Siffert: Appl. Phys. Lett. **62**, 979 (1993)
22. E.O. Sveinbjörnsson, O. Engström, U. Södervall: J. Appl. Phys. **73**, 7311 (1993)
23. R. Gafiteanu, U. Gösele, T.Y. Tan: *Mat. Res. Soc. Symp. Proc.* **378**, 297 (1995)
24. O. Porre, M. Stemmer, M. Pasquinelli: Materials Science and Engineering **B24**, 188 (1994)
25. M. Apel, I. Hanke, R. Schindler, W. Schröter: J. Appl. Phys. **76**, 4432 (1994)
26. S.M. Joshi, U.M. Gösele, T.Y. Tan: J. Appl. Phys. **77**, 3858 (1995)
27. S.A. McHugo, H. Hieslmair, E.R. Weber: In *Defects in Semiconductors 18, International Conference on Defects in Semiconductors*, edited by M. Suezawa and H. Katayama-Yoshida, Sendai, Japan, 1995, p. 1979
28. E.R. Weber, Appl. Phys. A **30**, 1 (1983)
29. E.O. Johnson: J. Appl. Phys. **28**, 1349 (1957)

30. A.M. Goodman: J. Appl. Phys. **32**, 2550 (1961)
31. J. Lagowski, A.M. Kontkiewicz, L. Jastrzebski, P. Edelman: Appl. Phys. Lett. **63**, 2902 (1993)
32. *ASTM Annual Book of Standards,* (ASTM, Metals Park, OH, 1983), p. 191
33. F.S. Ham: J. Phys. Chem. Solids **6**, 335 (1958)
34. D.G. Schimmel: Jour. Electrochem. Soc. **126**, 479 (1979)
35. *ASTM Annual Book of Standards,* (ASTM, Metals Park, OH, 1987), sec. 10, vol. 10/5, p. 63
36. *ASTM Annual Book of Standards,* (ASTM, Metals Park, OH, 1987), sec. 10, vol. 10/5, p. 620
37. L.C. Kimerling, J.L. Benton: Physica **116B**, 297 (1983)
38. G. Zoth, W. Bergholz: J. Appl. Phys. **67**, 6764 (1990)
39. H. Baker: In *Alloy Phase Diagrams*, vol. 3, (ASM International, 1992)
40. P. Villars, A. Prince, H. Okamoto: In *Handbook of Ternary Alloy Phase Diagrams*, vol. 3, (ASM International, 1995)
41. F. Shimura: Appl. Phys. Lett. **39**, 987 (1981)
42. L. Jastrzebski, P. Zanzucchi, D. Thebault, J. Lagowski: J. Elec. Chem. Soc. **129**, 1638 (1982)
43. G. Fraundorf, P. Fraundorf, R.A. Craven, R.A. Frederick, J. Moody, R.W. Shaw: J. Elec. Chem. Soc. **132**, 1701 (1985)
44. H.D. Chiou: J. Elec. Chem. Soc. **139**, 1680 (1992)
45. S. Ishikawa, M. Matsushita, J.-I. Shimomura: In *Defects in Semiconductors 18*, *International Conference on Defects in Semiconductors*, edited by M. Suezawa and H. Katayama-Yoshida, Sendai, Japan, 1995, p. 1823
46. W.K. Tice, T.Y. Tan: Mat. Res. Soc. Symp. Proc. **2**, 367 (1981)
47. D. Gilles, E.R. Weber, S.K. Hahn: Phys. Rev. Lett. **64**, 196 (1990)
48. S.A. McHugo, M. Mizuno, F.G. Kirscht, E.R. Weber: Appl. Phys. Lett. **66**, 2840 (1995)
49. K. Mahfoud, M. Loghmarti, J.C. Muller, P. Siffert: Mat. Sci. & Eng. B **36**, 63 (1996)
50. B. Shen, T. Sekiguchi, J. Jablonski, K. Sumino: J. Appl. Phys. **76**, 4540 (1994)